



Since January 2020 Elsevier has created a COVID-19 resource centre with free information in English and Mandarin on the novel coronavirus COVID-19. The COVID-19 resource centre is hosted on Elsevier Connect, the company's public news and information website.

Elsevier hereby grants permission to make all its COVID-19-related research that is available on the COVID-19 resource centre - including this research content - immediately available in PubMed Central and other publicly funded repositories, such as the WHO COVID database with rights for unrestricted research re-use and analyses in any form or by any means with acknowledgement of the original source. These permissions are granted for free by Elsevier for as long as the COVID-19 resource centre remains active.



Capacity of serotype 19A and 15B/C *Streptococcus pneumoniae* isolates for experimental otitis media: Implications for the conjugate vaccine

Alison S. Laufer^a, Jonathan C. Thomas^a, Marisol Figueira^b, Janneane F. Gent^c,
Stephen I. Pelton^b, Melinda M. Pettigrew^{a,*}

^a Division of Epidemiology of Microbial Diseases, Department of Epidemiology and Public Health, Yale University School of Medicine, New Haven, CT 06520, United States

^b Section of Pediatric Infectious Diseases, Boston Medical Center, Boston, MA 02118, United States

^c Center for Perinatal, Pediatric and Environmental Epidemiology, Department of Epidemiology and Public Health, Yale University School of Medicine, New Haven, CT 06520, United States

ARTICLE INFO

Article history:

Received 6 November 2009

Received in revised form

22 December 2009

Accepted 25 December 2009

Available online 10 January 2010

Keywords:

Streptococcus pneumoniae
Conjugate vaccine
qPCR assay

ABSTRACT

Non-vaccine *Streptococcus pneumoniae* serotypes are increasingly associated with disease. We evaluated isolates of the same sequence type (ST199) but different serotypes (15B/C, 19A) for growth *in vitro*, and pathogenic potential in a chinchilla otitis media model. We also developed a quantitative PCR (qPCR) assay to quantitatively assess each isolate, circumventing the need for selectable markers. *In vitro* studies showed faster growth of serotype 19A over 15B/C. Both were equally capable of colonization and middle ear infection in this model. Serotype 19A is included in new conjugate vaccine formulations while serotype 15B/C is not. Non-capsular vaccine targets will be important in disease prevention efforts.

© 2010 Elsevier Ltd. All rights reserved.

1. Introduction

Streptococcus pneumoniae, a major pathogen in children, causes a spectrum of clinically relevant infections from non-invasive, mucosal diseases such as acute otitis media (OM) to severe, invasive infections such as sepsis, bacteremic pneumonia and meningitis. Disease etiology and pathogenesis begin with nasopharyngeal colonization, which occurs in up to 65% of children [1,2]. *S. pneumoniae* is responsible for 20–50% of all middle ear infections in young children [3,4].

Current methods of control and prevention focus on the development of multivalent polysaccharide capsular vaccines designed to protect individuals against a subset of the more than 90 identified pneumococcal serotypes [5–7]. The heptavalent pneumococcal conjugate vaccine (PCV7) (Prenar, Wyeth) was licensed in 2000 to protect children and infants against seven serotypes (4, 6B, 9V, 14, 18C, 19F, 23F) responsible for the majority of pneumococcal infections [8].

Variability in the ability to cause site-specific disease has been reported not only among *S. pneumoniae* serotypes but also across

pneumococcal genetic backgrounds, as characterized by multilocus sequence typing [6,9–14]. The relative contribution of serotype and genetic background to disease potential is complex and not well defined. Sjöström et al. describe strains of different capsule types that act as either opportunistic pathogens in patients with underlying conditions (i.e. 11A, 19F, 23F) or as primary pathogens in healthy individuals (i.e. 1, 7F) [10]. In addition, strains from the same clonal complex that express different capsules have different disease potentials. For example, STO 9V-A with serotype 14 is more likely to act as a primary pathogen than STO 9V-A with serotype 19A [10]. Sabharwal et al. also demonstrate that two serotype 6A strains with different sequence types produce different disease patterns in the chinchilla model of experimental OM, further providing evidence that both capsule and non-capsule genes contribute to pneumococcal virulence [15].

Although the current vaccine is effective in preventing invasive pneumococcal disease caused by PCV7 serotypes, an equivalent level of protection against OM has not been observed [16,17]. Furthermore, the post-vaccine era has been characterized by a shift in the epidemiology of *S. pneumoniae* associated with OM. Among vaccinated children, the proportion of acute OM caused by non-vaccine serotypes and vaccine-related serotypes has increased since 2000 [17–21]. Capsule switching and expansion of non-vaccine serotypes have been proposed to explain these shifts in serotype-specific prevalence. As non-vaccine serotypes increase in prevalence, there has been a concomitant increase in antibi-

* Corresponding author at: Yale University, School of Public Health, 60 College Street, LEPH 816E, PO Box 208034, New Haven, CT 06520-8034, United States. Tel.: +1 203 785 5220; fax: +1 203 785 6130.

E-mail address: Melinda.Pettigrew@yale.edu (M.M. Pettigrew).

Table 1

Primers designed to create plasmid-based standard curves and to differentiate *S. pneumoniae* strains in mixed cultures. A larger 19A-specific fragment was cloned into TOPO vector pCR2.1 to increase cloning and transformation efficiency.

Strain of interest	Standard curve/qPCR	Primer	Sequence (5' → 3')	Amplicon size (bp)
FG23 ^{19A}	Standard curve	19A-f ^a 19A-r ^a	GTT AGT CCT GTT TTA GAT TTA TTT GGT GAT GT GAG CAG TCA ATA AGA TGA GAC GAT AGT TAG	478
	qPCR	<i>cps19AK</i> Forward <i>cps19AK</i> Reverse	CGG TGA CAC TAC GAC AAC TTA TGC TCG CAA ACC AGC TTC AAC AT	85
MIB02102 ^{15B/C}	Standard curve and qPCR	<i>wzy</i> Forward <i>wzy</i> Reverse	GCG GAT GAT TGT AGC GTT TT GAT TGT GTT CTG ATT CCT GCT C	195

^a Primers previously published by Pai et al. [23].

otic resistance among these strains [19,21,22]. One such lineage, ST199^{19A}, has been identified as responsible for a large proportion of replacement disease in the United States; serotype 19A is associated with multidrug resistance and ST199 is associated with penicillin resistance [21,23–25].

In order to protect against additional serotypes, vaccines in development are designed to cover a greater number of serotypes, including the 10-valent pneumococcal conjugate vaccine (PHiD-CV) and the CRM₁₉₇ 13-valent pneumococcal conjugate vaccine (PCV13) [26,27]. PHiD-CV includes serotypes 1, 5, and 7F in addition to those included in the PCV7; eight serotypes are conjugated to *Haemophilus influenzae* glycoprotein D, and one each to diphtheria toxin and tetanus toxin. PCV13 contains serotypes 1, 3, 5, 6A, 7F, and 19A in addition to the original seven serotypes [26], all conjugated to CRM₁₉₇. Serotype 19A has received considerable attention as an important expanding serotype and ST199 has been identified as a major lineage among serotype 19A strains but is also associated with capsule type 15B/C. Serotype 15B/C has also increased in prevalence among carriage and disease isolates since the introduction of PCV7 [28–32]. However, 15B/C was not included in the new PHiD-CV and PCV13 vaccines.

Understanding pneumococcal virulence requires disentangling the impact of capsular and non-capsular genetic contributions. Our goal is to compare clinically relevant strains of the same sequence type (ST) and different serotypes. We selected ST199^{19A} and ST199^{15B/C} strains to characterize in an experimental OM chinchilla model [12,15]. Most bacterial competition studies involve the transformation of strains with selectable markers, such as antibiotic resistance or carbon utilization genes; studies may also utilize spontaneous antibiotic resistant mutants [33–37]. Spontaneous mutations, selectable markers, laboratory manipulations, and passage of isolates potentially alter the fitness of bacteria [38–42]. In addition, while protocols have been adapted to transform unencapsulated and laboratory pneumococcal strains, many clinical isolates are difficult to transform. Pozzi et al. show that only 48% of the encapsulated strains were transformable, although all 42 encapsulated strains they tested carried competence genes [43]. Therefore, a second goal was to develop a quantitative PCR (qPCR) assay to compare the virulence potential of two strains by targeting innate genetic differences between strains. This assay allows for direct comparison of low passage, unmodified isolates and circumvents the need for inserting selectable markers.

2. Materials and methods

2.1. Bacterial strains, growth conditions, and growth rates

S. pneumoniae were grown at 35 °C, 5% CO₂, on trypticase yeast agar containing 5% sheep's blood (BD-Diagnostic Systems), or in Todd-Hewitt, 5% Yeast Extract liquid media. Strains used in this work were low passage carriage isolates selected from our *S. pneumoniae* collection. Strain FG23 is part of a collection of samples

taken from healthy children in a prospective study of pneumococcal carriage among PCV7 recipients in Texas between 2000 and 2001 [29]. Strain MIB02102 is from a collection of samples isolated from healthy children in a study of *S. pneumoniae* and *H. influenzae* colonization, and risk factors for carriage in children less than 3 years of age in Michigan [44]. Both strains belong to ST199. Strain FG23 is serotype 19A and strain MIB02102 is serotype 15B/C. While some studies consider 15B and 15C separately [45,46], the coding regions for serotypes 15B and 15C differ only by a single TA tandem repeat [47], which results in a single difference in the O-acetyl structure [28,47–49]. As serotypes 15B and 15C can interconvert, we consider 15B and 15C together in our analyses as is done in other studies [28,31,50]. Strains were typed previously by multilocus sequence typing [13] as described by Enright and Spratt [51].

2.2. Single strain growth rates *in vitro* and duration of colonization *in vivo*

To compare *in vitro* growth rates, FG23^{19A} and MIB02102^{15B/C} were grown as single strain liquid cultures, hereafter referred to as monocultures, at 35 °C. Over a 6-h period, 100 μl samples were plated on blood agar plates and incubated overnight to determine viable counts. Generation times were calculated by comparing the change in the log of colony forming units (CFU) over time.

To compare the duration of nasopharyngeal colonization *in vivo*, FG23^{19A} and MIB02102^{15B/C} were inoculated in the chinchilla model following protocols as previously described [15]. All chinchilla model experiments were carried out in accordance with Boston University Medical Center Institutional Animal Care and Use Committee guidelines. Female chinchillas (*Chinchilla laniger*) with no prior evidence of middle ear infection were used for this study. Nasopharyngeal washes were collected from chinchillas periodically to determine bacterial load by viable count (CFU/ml).

2.3. qPCR assay

Capsule encoding genes, *cps19AK* and *wzy* were targeted for differentiation between FG23^{19A} and MIB02102^{15B/C}, respectively [50]. Initially, PCR and qPCR were run on genomic DNA prepared from monocultures of each strain to ensure the primers selectively amplified the strain of interest and did not cross-react with the other strain. Plasmids were constructed with the TOPO TA Cloning Kit (Invitrogen) to carry the relevant gene target. Primers used in plasmid construction are listed in Table 1. Successful transformation was confirmed by PCR amplification of the gene fragment of interest and visualization of a band of the appropriate size on an agarose gel (2% in TBE buffer). Once confirmed, the DNA concentration was determined by spectrophotometer (OD₂₆₀) (Nanodrop, ThermoScientific) and the copy number was calculated using the formula from Dorak [52]. Plasmid preparations were diluted serially to create standard curves for quantitative analysis (log copy number versus cycle threshold (C_t)), which span approximately 10³

to 10^8 copies. Plasmid-based standard curves were validated using viable colony count data.

DNA was extracted from each mixed FG23^{19A}/MIB02102^{15B/C} sample using the QIAamp DNA Minikit (QIAGEN) according to the manufacturer's instructions, with one modification: elution of DNA into 50 μ l. Genomic DNA from each mixed sample underwent two separate qPCR reactions – one with each of the primer sets designed for differentiation of the pair. See Table 1 for qPCR primers. qPCR was completed using the Mx3005P (Stratagene) and SYBR Green 2x Master Mix (Applied Biosystems). Cycling conditions for qPCR were: 95 °C for 15 min followed by 35 cycles of 94 °C for 20 s, 55 °C for 20 s, and 72 °C for 20 s. Standard curves were run in parallel to the unknown samples. Dissociation curves were completed to check for absence of primer dimers. qPCR was always done in duplicate and negative controls were included in every set of reactions. The plasmid-based standard curves were used to determine number of CFU per strain in mixed cultures. The competitive fitness index was selected to measure strain composition in mixed cultures [35]. Competitive fitness index was calculated by strain ratio of output divided by strain ratio of input [35].

2.4. qPCR assay validation

To validate the qPCR assay, *in vitro* monocultures of FG23^{19A} and MIB02102^{15B/C} incubated at the stated conditions were combined in different, known amounts to create mixed cultures, and processed for the qPCR assay as described above. Monocultures were grown overnight to determine the viable count in each monoculture, as well as the CFU/strain added to each mixed culture. These data served as the gold standard for comparisons to results calculated by the qPCR assay. Using monoculture viable count data and the standard curve equations calculated by least squares linear regression, expected C_t 's were determined for all samples. Expected C_t 's were compared to the observed C_t 's and relative error percents were calculated to assess accuracy. The *in vitro* mixed culture experiment was repeated three times.

2.5. Assessing strain potential *in vitro* and *in vivo*

To compare growth characteristics *in vitro*, monocultures of each strain pair were grown for 2.5 h, mixed in fresh liquid media, and allowed to co-incubate for 5 h to assess strain composition using the described qPCR assay. Each experiment was repeated three times.

For chinchilla model experiments, protocols from Sabharwal et al. [15] were followed with minor alterations. Strains were grown as monocultures and mixed in a 1:1 ratio just prior to inoculating the nares of healthy chinchillas. Nasopharyngeal washes were collected from all chinchillas on days 1 and 5 before barotrauma. Barotrauma was then performed to create negative pressure in the middle ear cavity and enhance development of experimental OM by aspirating up to 250 μ l of air with a 25-gauge needle from the middle ear through the bullar bone. Tympanometry was used to confirm development of negative pressure in the middle ear space. Chinchillas were monitored closely for development of experimental OM by otomicroscopy and tympanometry. Once a chinchilla presented with symptoms of experimental OM infection, the middle ear cavity was opened. Both middle ear and nasopharyngeal lavage samples were collected at this time. Microbial DNA was extracted from nasopharyngeal lavages and middle ear cavity samples as described above. The qPCR assay was performed on the genomic DNA extracted from the samples to determine which strain was more robust in colonizing the nasopharynx and/or establishing infection in the middle ear space. Total viable counts were completed by plating on blood agar overnight and compared with

total bacterial loads determined by qPCR. Relative error percents were calculated by comparing viable count and qPCR data for each chinchilla at each time point and tissue source (nasopharyngeal lavage or middle ear sample). In addition, serotyping by Quellung reaction was also completed [53] by plating on blood agar overnight and determining serotype for a small sample of colonies from each chinchilla to confirm that the qPCR assay was detecting the correct serotype in the chinchilla model samples. The experimental OM co-culture inoculum experiment was completed three times with 6, 6, and 4 chinchillas, respectively.

2.6. Statistical analyses

All statistical analyses used SAS 9.1 (SAS Institute, Cary, NC). In addition to descriptive statistics for each experiment, Kappa statistics were calculated to evaluate the qPCR assay's ability to predict the dominant serotype as determined by Quellung serotyping reaction. Non-parametric and parametric methods were used for analysis of the chinchilla model data. Kaplan–Meier survival tests were used to determine if the duration of colonization differed between the two strains. *t*-tests were used to determine if FG23^{19A} was more capable of causing infection than MIB02102^{15B/C} in the experimental OM infections.

3. Results

3.1. Single strain growth rates *in vitro* and duration of colonization *in vivo*

FG23^{19A} had a shorter generation time than isolate MIB02102^{15B/C}. FG23^{19A} doubled every 54.3 min, whereas MIB02102^{15B/C} doubled every 69.2 min (Fig. 1A). To compare the duration of colonization, chinchillas were inoculated with either FG23^{19A} or MIB02102^{15B/C}. All chinchillas were successfully colonized and cleared the bacteria on or before day 20 (Fig. 1B). Bacterial loads were calculated on days 1, 5, 8, 12, 15, and 20 and there were no significant differences in bacterial load between FG23^{19A}- and MIB02102^{15B/C}-colonized chinchillas on any given day, $P > 0.5$. There were no statistically significant differences between the groups in duration of colonization (Kaplan–Meier, $P = 0.18$).

3.2. qPCR assay design validation

Overall assessment of the standard curves used in the qPCR assay showed a linear relationship between the log 10 of the plasmid copy number and the observed C_t 's ($R^2 > 0.95$). Amplification efficiencies were calculated using the formula $E = 10^{[1/-\text{slope}]}$ [54], and ranged from 1.9 to 2.3, within the range considered acceptable and consistent with other studies [54–57]. Intraassay and interassay variability were slight (data not shown).

Viable count data were used as the gold standard for assay validation. Monocultures were analyzed by viable count (CFU/ml) and by qPCR (C_t) to assess the assay's accuracy in single strain and mixed cultures. The mean relative percent errors were 7.28% (SD: 6.35, Median: 5.36%) for the serotype 19A plasmid-based standard curve, 7.63% (SD: 6.47, Median: 6.5%) for the 15B/C plasmid-based standard curve.

3.3. *In vitro* growth characteristics, and *in vivo* capacity to colonize and infect

We first assessed co-culture growth characteristics *in vitro* using a range of mixed culture input ratios. When the two strains were allowed to co-incubate *in vitro*, FG23^{19A} consistently outgrew

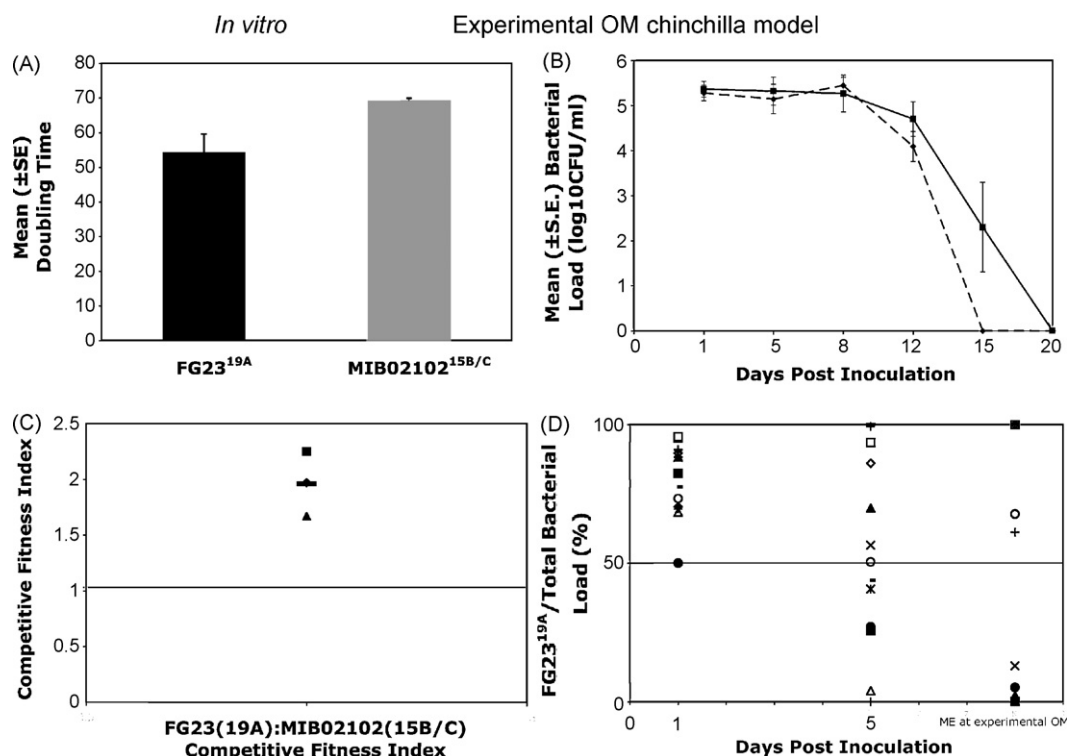


Fig. 1. Bacterial strains in monoculture *in vitro* (A) and the experimental OM model (B); in co-culture *in vitro* (C) and co-inoculated into the experimental OM model (D). (A) Mean (SE) doubling time (minutes) of MIB02102^{15B/C} and FG23^{19A}. (B) Chinchilla OM model, single strain duration of colonization, median (SE) nasopharyngeal bacterial load time course (log₁₀(CFU/ml)), MIB02102^{15B/C} ($n = 4$) (dashed line), FG23^{19A} ($n = 3$) (solid line). No bacteria detected at day 15 or 20 for MIB02102^{15B/C}-colonized chinchillas, no bacteria detected at day 20 for FG23^{19A}-colonized chinchillas. (C) *In vitro* competitive fitness index calculated by dividing the output FG23^{19A}:MIB02102^{15B/C} ratio by the input FG23^{19A}:MIB02102^{15B/C} ratio. Values over 1.0 indicate FG23^{19A} was more prevalent by qPCR. Different symbols represent different experiment repeats; black bar is the mean value. (D) Experimental OM co-inoculation. Data shown represent the percent of FG23^{19A} in the total sample over the course of colonization and infection. Values over 50% indicate FG23^{19A} was the more dominant strain, below 50% indicate MIB02102^{15B/C} was more dominant. In the middle ear sample at experimental OM, 7/14 chinchillas had MIB02102^{15B/C} dominating the infection and 7/14 chinchillas had FG23^{19A} dominating the infection. Each marker represents a different chinchilla over the course of infection.

MIB02102^{15B/C}, with a mean (SE) competitive fitness index of 1.96 (0.167) (Fig. 1C and Table 2).

To assess capacity to colonize and to infect in the experimental OM model, chinchillas were inoculated with a 1:1 ratio and nasopharyngeal samples were collected on days 1 and 5. On day 1, all chinchillas were positive for *S. pneumoniae* by culture and qPCR analyses. Fourteen of 16 chinchillas developed symptoms of experimental OM (4 chinchillas on day 7 and 10 on day 8). Fig. 1D shows the FG23^{19A} versus MIB02102^{15B/C} capacity to colonize the nasopharynx and infect the middle ear in the experimental OM model. Quellung reaction serotyping was completed on a sample of colonies from each nasopharyngeal and middle ear sample from each chinchilla to determine the more prevalent serotype. These data significantly matched the qPCR data, according to dominant serotype in each sample (Kappa statistic 0.77, $P < 0.001$). Mean total bacterial load (log₁₀(CFU/ml)) as calculated by qPCR assay and viable count were compared (Fig. 2). Overall, percent relative error of the assay was 9.51%. For nasopharyngeal samples taken on days 1, 5, and at the time of experimental OM onset, percent relative error was 8.5%, 8.82%, and 12.78%, respectively (Fig. 2). Percent rel-

ative error for middle ear samples total bacterial load was 7.39% (Fig. 2).

3.4. Nasopharyngeal colonization

Initially FG23^{19A} outcompeted MIB02102^{15B/C} in the nasopharyngeal cavity (paired two-tailed t -test, $P < 0.0001$). On day 1, 94% (15/16) of the nasopharyngeal cavities were colonized with more FG23^{19A} than MIB02102^{15B/C}. However, by day 5 this disparity was reduced, with MIB02102^{15B/C} being more prevalent in 43.75% (7/16) of the nasopharyngeal samples (paired two-tailed t -test, $P = 0.409$).

3.5. Middle ear infection

The middle ear cavity was sampled upon onset presentation of experimental OM symptoms after barotrauma. For four chinchillas, this was 2 days after barotrauma (day 7), and was 3 days after barotrauma (day 8) for the remaining 10 chinchillas. Of the 14 chinchillas that developed experimental OM, 50% (7/14) had

Table 2

In vitro growth characteristics. Competitive fitness index values greater than 1.0 indicate FG23^{19A} was doubling faster than MIB02102^{15B/C}.

Input ratio (FG23 ^{19A} : MIB02102 ^{15B/C})	Output ratio (FG23 ^{19A} : MIB02102 ^{15B/C})	Competitive fitness index Output ratio:input ratio
1.00:1.0	1.67:1.0	1.67
1.00:1.5	1.32:1.0	1.97
2.37:1.0	5.33:1.0	2.25

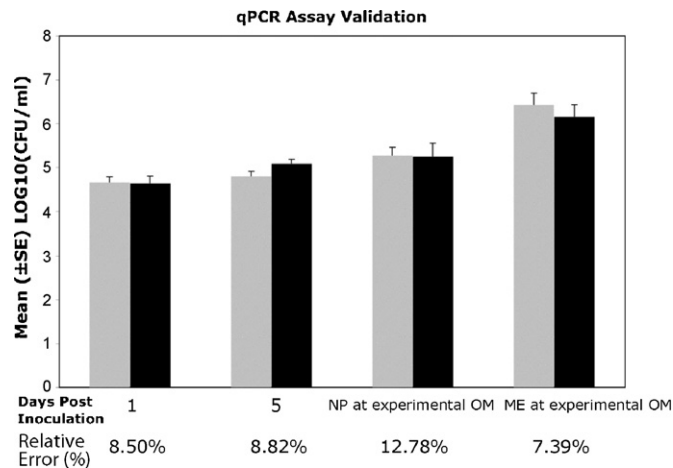


Fig. 2. Mean total bacterial load (log₁₀(CFU/ml)) over the course of colonization and infection in the chinchilla model as calculated by qPCR assay (shaded) and by viable count method (black). Percent relative error was determined by comparing total bacterial load calculated by the two methods for each chinchilla at each time point and tissue source. Days 1, 5, and nasopharyngeal (NP) at experimental OM are from nasopharyngeal samples; ME at experimental OM is from middle ear samples at onset of experimental OM.

FG23^{19A} dominating the middle ear infection. Thus, neither strain was able to outcompete the other (paired *t*-test for strain composition, $P=0.779$). Fig. 1D shows the strain composition over the course of colonization and infection. Overall, in the middle ear samples, the percent FG23^{19A} ranged from 0.03% to 100%, mean 46.42% (SD 46.69%) (Fig. 1D). Median weight did not differ between the two groups presenting with experimental OM symptoms on days 7 and 8 (Wilcoxon Rank Sum test, $P=0.5$). The dominant strain in middle ear samples matched the dominant bacteria in 12 of 14 nasopharyngeal samples.

4. Discussion

We evaluated two clinically relevant pneumococcal strains *in vitro* and in a chinchilla model of disease. We hypothesized that FG23^{19A} would outcompete MIB02102^{15B/C} in the chinchilla model as it does *in vitro*. However, our data indicate that both 19A and 15B/C strains of ST199 have similar pathogenic potential in experimental OM. The observation that serotypes previously classified as having lower invasive potential (i.e. 15B/C) have similar capacity to produce experimental OM as serotypes classified as having greater disease potential (i.e. 19A) has implications for the effectiveness of PCV7, PHiD-CV, and PCV13 in preventing otitis media and possibly non-bacteremic pneumonia.

Both capsule type and genetic background contribute to disease potential and presentation [10]. Current methods of prevention and control focus on the polysaccharide capsule, an important pneumococcal virulence factor. Surprisingly, PCV7 has not reduced nasopharyngeal carriage of *S. pneumoniae* but has resulted in complete replacement, with virtually the same prevalence of pneumococcal carriage, of non-vaccine serotypes [17–21]. With over 90 different serotypes expressed and high levels of genomic plasticity, researchers cannot accurately predict which pneumococcal serotypes are likely to produce mucosal and/or invasive disease and which will be important to include in future vaccines.

Second generation vaccines in development include serotypes 1, 3, 5, 6A, 7F, and 19A. Serotypes 3, 6A, and 19A are common middle ear pathogens [27]. Recent studies identified capsule type 19A as an important expanding serotype [21–24] and inclusion of 19F capsular polysaccharide in the currently licensed vaccine formu-

lation, PCV7, has not provided cross-protection against serotype 19A-associated disease [23]. Although serogroups 1, 5, and 7 are common invasive pneumococcal disease pathogens worldwide [58], these are rarely associated with OM [27]. Therefore PHiD-CV may provide only minimal improvement over the PCV7 in preventing pneumococcal OM.

Minor differences between serotype 19A strains and serotype 15B/C strains may explain why serotype 19A has expanded more quickly than serotype 15B/C over the last decade. These differences include a shorter generation time observed in serotype 19A. Shouval et al. reported a slight increase in the odds of finding serotype 19A in disease compared to carriage (versus no different than 1.0 in serotype 15B/C) [9]. Epidemiological data suggest that serogroup 15 strains are increasing in carriage and disease [21,23,24,28–32,59]. Between 2001 and 2007, Huang et al. observed a statistically significant increase in 19A colonization and a 50% increase, though not significant, in 15B/C colonization [31]. Casey et al. recovered both serotypes 19A and 15B/C from the middle ear space of children with and without acute OM [59,60]. The most common serotypes recovered were 19A, 11, 15, and 23B from non-acute OM visits and 19A, 15, and 6C from acute OM visit [59]. Hicks et al. found statistically significant increases in the rates of invasive pneumococcal disease due to 19A and 15 in young children and older adults after the introduction of PCV7 in the United States [32]. Gonzalez et al. reported a significant increase in invasive pneumococcal disease caused by serogroup 15, with ST199 being the predominant clone [28].

FG23^{19A} appeared more robust than MIB02102^{15B/C} only *in vitro*. In the experimental OM model, we show that FG23, which expresses a 19A capsule, does not have a significant advantage over a serotype 15B/C strain, MIB02102, in its ability to colonize or cause disease. This is consistent with observations that 19A and 15B/C are two of the most prevalent serotypes found in the nasopharynx of children [31]. As serotype 19A isolates are recovered more frequently than serotype 15B/C from children with invasive pneumococcal disease, yet colonization appears similar, tissue-specific genetic requirements beyond capsule are potentially responsible for differences in colonization, mucosal infection, and bloodstream invasion.

Weinberger et al. [61] proposed that the metabolic costs of specific polysaccharide capsules could be used to predict the emergence of individual pneumococcal serotypes. These authors postulate that there is a greater metabolic cost to produce capsule in serotypes with more carbons and high-energy bonds per polysaccharide repeat unit. Thus, serotypes with low production costs are increasing in prevalence because they can produce more polysaccharide capsule and are consequently better able to evade neutrophil-mediated killing. Data indicate that serotype 15B/C has more carbons and high-energy bonds per repeat unit than serotype 19A [61]. The shorter generation time of FG23^{19A} over MIB02102^{15B/C} found here supports this “cost of capsule” model. Serotype 19A has 7 high energy bonds and 20 carbons, whereas serotype 15B/C has 11.4 high energy bonds and 15B and 15C have 33.4 and 32 carbons, respectively. Weinberger et al. did not directly examine the degree of encapsulation and neutrophil-mediated killing of serotype 15 strains [61]. Based on their results, we would also expect that FG23^{19A} would persist longer in carriage and would be a better competitor in the disease model because it can produce more capsule for the same energy cost and thus should be able to evade destruction by the immune system. However, our chinchilla model did not identify significant differences between the two serotypes when inoculated in monoculture or in co-culture. Although a small number of animals were studied for duration of colonization, we utilized a non-parametric test appropriate for the small number and expect any differences in duration of colonization would be slight.

These data further confirm that serotype is not the sole factor in determining prevalence in carriage or virulence potential. Other factors contribute to virulence in disease models and in patients with pneumococcal disease, including pneumococcal genetic background, doubling time, pathogenicity islands, prevalence in the population, and host factors [62–65]. There is evidence that genetic background, beyond clonal complex and serotype, influence pneumococcal disease potential [10,65,66]. *S. pneumoniae* is a highly plastic species with a high level of genetic diversity. Accessory genes exist within the pneumococcal supragenome, which may cluster into regions [66]. Accessory regions vary not only between, but also within clonal types. These accessory regions may also encode redundant functions, i.e. phosphotransferase sugar transport systems and ATP-binding cassette transport systems [66]. This redundancy suggests that a single gene or gene profile will not necessarily identify strains that are more or less pathogenic. A more complete understanding of the pneumococcal supragenome, including accessory regions, serotype, and clonal complex, when combined with epidemiological and clinical data will help elucidate disease potential.

Although the chinchilla model does not use a genetically pure line of chinchillas, this is outweighed by its usefulness in closely mirroring middle ear disease in young children. An advantage to this model is that it allows nasopharyngeal colonization to be established before infection, further improving upon previous chinchilla models of experimental OM which used direct middle ear inoculation [12,15]. Following colonization, barotrauma created negative pressure in the middle ear cavity, allowing bacteria into the middle ear space and leading to infection. Eustachian tube dysfunction in humans is often caused by a viral upper respiratory tract infection. Influenza, RSV, coronavirus, and adenovirus are associated with otitis media [67] but may differentially impact Eustachian tube function [68–70]. Rather than choosing one particular virus, we used barotrauma to create the negative pressure, which enabled us to reproduce the Eustachian tube dysfunction in a consistent, simplified manner. Day of barotrauma may affect the outcome of experimental OM. In the literature challenge to the middle ear via barotrauma or bacterial inoculation varies from 48 h to 7 days [15,71,72]. We selected day 5 for barotrauma to allow bacterial colonization to be established before infection and also to reflect peak incidence of acute OM following upper respiratory tract infection in children which occurs on days 3 and 5 [73].

We developed a culture-independent assay to measure mixed culture strain composition. Generally, competition studies rely on spontaneous mutations or selectable markers in laboratory-altered strains for differentiation. However, these markers may introduce artificial fitness costs not found in the parent strain [38–42,74]. By using viable count data and Quellung reaction serotyping data, we showed the qPCR assay is selectively and accurately amplifying the *S. pneumoniae* strains in monoculture, and in mixed cultures *in vitro* and in the chinchilla model of disease. To our knowledge, this is the first qPCR assay to take advantage of innate genetic divergences for differentiation between strains of the same species in order to measure *in vitro* growth characteristics and *in vivo* capacity. Traditionally, serotype assignment is completed on a limited number of colony forming units. Serotyping several hundred colonies per sample per animal is inefficient, costly, and impractical. The qPCR assay uses the larger sample and provides definitive, quantitative results. The ability to assess capacity to colonize and to cause experimental OM in the disease model will assist in the search for virulence factors in *S. pneumoniae* strains. In addition, the assay may be adapted for use with other bacterial species.

As with any assay, there are limitations to our method for assessing growth characteristics and infection potential. If the bacterial load in the chinchilla model is low, there is a limit of detection in qPCR. Also, it is possible to overload the qPCR with too much

template [75]. The simplest solutions are to decrease the volume of template added or to dilute the template. We found a 5-fold dilution was sufficient when saturation was a problem. qPCR does not provide a method for differentiating between metabolically active and inactive bacteria. We cannot definitely state whether the viable count data are yielding 100% of the live bacteria present in the sample or whether the qPCR assay is overestimating absolute bacterial counts by detecting DNA from dead bacteria. Conversely, researchers have demonstrated the presence of viable bacteria in culture-negative middle ear samples [76,77]. Therefore, the assay provides a culture-independent method, which may be more accurate than culture methods. Post et al. have shown that after 3 days, DNA from dead bacteria in the chinchilla middle ear is no longer amplifiable [77]. In addition, the qPCR analyses are dependent upon plasmid-based standard curve copy number calculations, which could contribute to either underestimation or overestimation of viable count. In this project, data from viable count and qPCR analyses were comparable. These limitations regarding detection of viable bacteria must be taken into consideration when evaluating absolute viable counts. This may be less of a problem here, when comparing strain relative ratios.

Despite these limitations, we believe our qPCR assay, when designed properly, provides a convenient, accurate, novel method for comparing closely related clinical isolates. The assay was designed to be easily adapted for use with other pneumococcal strains as well as other bacterial species with genomic plasticity, such as *H. influenzae*, *Pseudomonas aeruginosa*, *Escherichia coli*, and *Staphylococcus aureus* [78–80]. The assay's ability to compare closely related strains of pneumococci without laboratory-based manipulations makes it a useful tool for evaluating virulence potential in the search for putative virulence factors among clinical isolates.

Data reported here, along with the observations that serogroup 15 is increasing in nasopharyngeal carriage, otitis media, and invasive disease all suggest that serotype 15B/C may soon become an important cause of pneumococcal disease [29–32]. Shouval et al. describe that the likelihood of finding serotype 15B/C strains in invasive disease or acute OM following colonization is equal to finding it in carriage [9]. Therefore, as the prevalence of 15B/C carriage increases, serotype 15B/C strains may become responsible for more disease. Continually adding serotypes to the current vaccines is not a sustainable approach to prevention and control of pneumococcal disease. As both serotypes 15B/C and 19A were demonstrated to be virulent in our experimental OM model, further evaluation of non-vaccine serotypes to determine their capacity to colonize and produce acute OM is needed to understand the potential impact of next generation capsular vaccines. Further research is needed to identify other non-capsule virulence factors and to develop alternative strategies for prevention and control.

Acknowledgements

We thank Kristopher Fennie (Yale School of Nursing) for helpful discussions and input. We also thank Loc Truong, Abbie Stevenson, and Jonathan Gaskins (Boston Medical Center) for their expert assistance with the experimental otitis media chinchilla model. Pneumococcal strains were kindly provided by Betsy Foxman and Faryal Ghaffar.

The National Institute of Allergy and Infectious Diseases provided funding for this research (R01 A1068043 to M.M.P.).

References

- [1] Syrjanen RK, Kilpi TM, Kaijalainen TH, Herva EE, Takala AK. Nasopharyngeal carriage of *Streptococcus pneumoniae* in Finnish children younger than 2 years old. *J Infect Dis* 2001;184(4):451–9.

- [2] Dagan R, Givon-Lavi N, Zamir O, Fraser D. Effect of a nonavalent conjugate vaccine on carriage of antibiotic-resistant *Streptococcus pneumoniae* in day-care centers. *Pediatr Infect Dis J* 2003;22(6):532–40.
- [3] Casey JR, Pichichero ME. Changes in frequency and pathogens causing acute otitis media in 1995–2003. *Pediatr Infect Dis J* 2004;23(9):824–8.
- [4] Bluestone CD, Stephenson JS, Martin LM. Ten-year review of otitis media pathogens. *Pediatr Infect Dis J* 1992;11(8 Suppl.):S7–11.
- [5] Tuomanen EI. The pneumococcus. Washington, DC: ASM Press; 2004.
- [6] Sandgren A, Sjöstrom K, Olsson-Liljequist B, Christensson B, Samuelsson A, Kronvall G, et al. Effect of clonal and serotype-specific properties on the invasive capacity of *Streptococcus pneumoniae*. *J Infect Dis* 2004;189(5):785–96.
- [7] Briles DE, Crain MJ, Gray BM, Forman C, Yother J. Strong association between capsular type and virulence for mice among human isolates of *Streptococcus pneumoniae*. *Infect Immun* 1992;60(1):111–6.
- [8] Overturf G. Preliminary guidelines on new PVC7 vaccine released by ACIP. *Am Acad Pediatr News* 2000;16(4), 1a–6.
- [9] Shouval D, Greenberg D, Givon-Lavi N, Porat N, Dagan R. Site-specific disease potential of individual *Streptococcus pneumoniae* serotypes in pediatric invasive disease, acute otitis media and acute conjunctivitis. *Pediatr Infect Dis J* 2006;25(7):602–7.
- [10] Sjöström K, Spindler C, Ortqvist A, Kalin M, Sandgren A, Kühlmann-Berenzon S, et al. Clonal and capsular types decide whether pneumococci will act as a primary or opportunistic pathogen. *Clin Infect Dis* 2006;42(4):451–9.
- [11] Obert C, Sublett J, Kaushal D, Hinojosa E, Barton T, Tuomanen EI, et al. Identification of a candidate *Streptococcus pneumoniae* core genome and regions of diversity correlated with invasive pneumococcal disease. *Infect Immun* 2006;74(8):4766–77.
- [12] Forbes ML, Horsey E, Hiller NL, Buchinsky FJ, Hayes JD, Compliment JM, et al. Strain-specific virulence phenotypes of *Streptococcus pneumoniae* assessed using the *Chinchilla laniger* model of otitis media. *PLoS ONE* 2008;3(4):e1969.
- [13] Pettigrew M, Fennie K, York M, Daniels J, Ghaffar F. Variation in the presence of neuraminidase genes among *Streptococcus pneumoniae* isolates with identical sequence types. *Infect Immun* 2006;74(6):3360–5.
- [14] Pettigrew M, Fennie K. Genomic subtraction followed by dot blot screening of *Streptococcus pneumoniae* clinical and carriage isolates identifies genetic differences associated with strains that cause otitis media. *Infect Immun* 2005;73(5):2805–11.
- [15] Sabharwal V, Ram S, Figueira M, Park IH, Pelton SI. Role of complement in host defense against pneumococcal otitis media. *Infect Immun* 2009;77(3):1121–7.
- [16] Black S, Shinefield H, Fireman B, Lewis E, Ray P, Hansen JR, et al. Efficacy, safety and immunogenicity of heptavalent pneumococcal conjugate vaccine in children. Northern California Kaiser Permanente Vaccine Study Center Group. *Pediatr Infect Dis J* 2000;19(3):187–95.
- [17] Eskola J, Kilpi T, Palmu A, Jokinen J, Haapakoski J, Herva E, et al. Efficacy of a pneumococcal conjugate vaccine against acute otitis media. *N Engl J Med* 2001;344(6):403–9.
- [18] Pelton S, Loughlin A, Marchant C. Seven valent pneumococcal conjugate vaccine immunization in two Boston communities: changes in serotypes and antimicrobial susceptibility among *Streptococcus pneumoniae* isolates. *Pediatr Infect Dis J* 2004;23(11):1015–22.
- [19] McEllistrem M, Adams J, Patel K, Mendelsohn A, Kaplan S, Bradley J, et al. Acute otitis media due to penicillin-nonsusceptible *Streptococcus pneumoniae* before and after the introduction of the pneumococcal conjugate vaccine. *Clin Infect Dis* 2005;40(12):1738–44.
- [20] McEllistrem M, Adams J, Mason E, Wald E. Epidemiology of acute otitis media caused by *Streptococcus pneumoniae* before and after licensure of the 7-valent pneumococcal protein conjugate vaccine. *J Infect Dis* 2003;188(11):1679–84.
- [21] Pichichero M, Casey J. Emergence of a multiresistant serotype 19A pneumococcal strain not included in the 7-valent conjugate vaccine as an otopathogen in children. *JAMA* 2007;298(15):1772–8.
- [22] Choi EH, Kim SH, Eun BW, Kim SJ, Kim NH, Lee J, et al. *Streptococcus pneumoniae* serotype 19A in children, South Korea. *Emerg Infect Dis* 2008;14(2):275–81.
- [23] Pai R, Moore MR, Pilishvili T, Gertz RE, Whitney CG, Beall B, et al. Postvaccine genetic structure of *Streptococcus pneumoniae* serotype 19A from children in the United States. *J Infect Dis* 2005;192(11):1988–95.
- [24] Brueggemann A, Pai R, Crook D, Beall B. Vaccine escape recombinants emerge after pneumococcal vaccination in the United States. *PLoS Pathog* 2007;3(11):e168.
- [25] Messina AF, Katz-Gaynor K, Barton T, Ahmad N, Ghaffar F, Rasko D, et al. Impact of the pneumococcal conjugate vaccine on serotype distribution and antimicrobial resistance of invasive *Streptococcus pneumoniae* isolates in Dallas, TX, children from 1999 through 2005. *Pediatr Infect Dis J* 2007;26(6):461–7.
- [26] Shouval DS, Greenberg D, Givon-Lavi N, Porat N, Dagan R. Serotype coverage of invasive and mucosal pneumococcal disease in Israeli children younger than 3 years by various pneumococcal conjugate vaccines. *Pediatr Infect Dis J* 2009;28(4):277–82.
- [27] Rodgers GL, Arguedas A, Cohen R, Dagan R. Global serotype distribution among *Streptococcus pneumoniae* isolates causing otitis media in children: potential implications for pneumococcal conjugate vaccines. *Vaccine* 2009;27(29):3802–10.
- [28] Gonzalez BE, Hulten KG, Lamberth L, Kaplan SL, Mason Jr EO, U.S. Pediatric Multicenter Pneumococcal Surveillance Group. *Streptococcus pneumoniae* serogroups 15 and 33: an increasing cause of pneumococcal infections in children in the United States after the introduction of the pneumococcal 7-valent conjugate vaccine. *Pediatr Infect Dis J* 2006;25(4):301–5.
- [29] Ghaffar F, Barton T, Lozano J, Muniz LS, Hicks P, Gan V, et al. Effect of the 7-valent pneumococcal conjugate vaccine on nasopharyngeal colonization by *Streptococcus pneumoniae* in the first 2 years of life. *Clin Infect Dis* 2004;39(7):930–8.
- [30] Byington CL, Samore MH, Stoddard GJ, Barlow S, Daly J, Korgenski K, et al. Temporal trends of invasive disease due to *Streptococcus pneumoniae* among children in the intermountain west: emergence of nonvaccine serogroups. *Clin Infect Dis* 2005;41(1):21–9.
- [31] Huang SS, Hinrichsen VL, Stevenson AE, Rifas-Shiman SL, Kleinman K, Pelton SI, et al. Continued impact of pneumococcal conjugate vaccine on carriage in young children. *Pediatrics* 2009;124(1):e1–11.
- [32] Hicks LA, Harrison LH, Flannery B, Hadler JL, Schaffner W, Craig AS, et al. Incidence of pneumococcal disease due to non-pneumococcal conjugate vaccine (PCV7) serotypes in the United States during the era of widespread PCV7 vaccination, 1998–2004. *J Infect Dis* 2007;196(9):1346–54.
- [33] Roos V, Ulett GC, Schembri MA, Klemm P. The asymptomatic bacteriuria *Escherichia coli* strain 83972 outcompetes uropathogenic *E. coli* strains in human urine. *Infect Immun* 2006;74(1):615–24.
- [34] Janakiraman A, Schlauch JM. The putative iron transport system SitABCD encoded on SPI1 is required for full virulence of *Salmonella typhimurium*. *Mol Microbiol* 2000;35(5):1146–55.
- [35] Brickman TJ, Vanderpool CK, Armstrong SK. Heme transport contributes to *in vivo* fitness of *Bordetella pertussis* during primary infection in mice. *Infect Immun* 2006;74(3):1741–4.
- [36] Laufer AS, Siddall ME, Graf J. Characterization of the digestive-tract microbiota of *Hirudo orientalis*, a European medicinal leech. *Appl Environ Microbiol* 2008;74(19):6151–4.
- [37] Armalyte J, Seputiene V, Melefors O, Suziedeliene E. An *Escherichia coli* ar mutant has decreased fitness during colonization in a mouse model. *Res Microbiol* 2008;159(6):486–93.
- [38] Johnson CN, Briles DE, Benjamin Jr WH, Hollingshead SK, Waites KB. Relative fitness of fluoroquinolone-resistant *Streptococcus pneumoniae*. *Emerg Infect Dis* 2005;11(6):814–20.
- [39] Andersson DI, Levin BR. The biological cost of antibiotic resistance. *Curr Opin Microbiol* 1999;2(5):489–93.
- [40] Andersson DI. The biological cost of mutational antibiotic resistance: any practical conclusions? *Curr Opin Microbiol* 2006;9(5):461–5.
- [41] Baneyx F. Recombinant protein expression in *Escherichia coli*. *Curr Opin Biotechnol* 1999;10(5):411–21.
- [42] Bjorkholm B, Sjolund M, Falk PG, Berg OG, Engstrand L, Andersson DI. Mutation frequency and biological cost of antibiotic resistance in *Helicobacter pylori*. *Proc Natl Acad Sci U S A* 2001;98(25):14607–12.
- [43] Pozzi G, Masala L, Iannelli F, Manganelli R, Havarstein L, Piccoli L, et al. Competence for genetic transformation in encapsulated strains of *Streptococcus pneumoniae*: two allelic variants of the peptide pheromone. *J Bacteriol* 1996;178(20):6087–90.
- [44] Farjo RS, Foxman B, Patel MJ, Zhang L, Pettigrew MM, McCoy SI, et al. Diversity and sharing of *Haemophilus influenzae* strains colonizing healthy children attending day-care centers. *Pediatr Infect Dis J* 2004;23(1):41–6.
- [45] Sleeman KL, Griffiths D, Shackley F, Diggle L, Gupta S, Maiden MC, et al. Capsular serotype-specific attack rates and duration of carriage of *Streptococcus pneumoniae* in a population of children. *J Infect Dis* 2006;194(5):682–8.
- [46] Arguedas A, Dagan R, Guevara S, Porat N, Soley C, Perez A, et al. Middle ear fluid *Streptococcus pneumoniae* serotype distribution in Costa Rican children with otitis media. *Pediatr Infect Dis J* 2005;24(7):631–4.
- [47] van Selm S, van Cann LM, Kolkman MA, van der Zeijst BA, van Putten JP. Genetic basis for the structural difference between *Streptococcus pneumoniae* serotype 15B and 15C capsular polysaccharides. *Infect Immun* 2003;71(11):6192–8.
- [48] Bentley SD, Aanensen DM, Mavroidi A, Saunders D, Rabinowitsch E, Collins M, et al. Genetic analysis of the capsular biosynthetic locus from all 90 pneumococcal serotypes. *PLoS Genet* 2006;2(3):e31.
- [49] Jansson PE, Lindberg B, Lindquist U, Ljungberg J. Structural studies of the capsular polysaccharide from *Streptococcus pneumoniae* types 15B and 15C. *Carbohydr Res* 1987;162(1):111–6.
- [50] Pai R, Gertz RE, Beall B. Sequential multiplex PCR approach for determining capsular serotypes of *Streptococcus pneumoniae* isolates. *J Clin Microbiol* 2006;44(1):124–31.
- [51] Enright MC, Spratt BG. A multilocus sequence typing scheme for *Streptococcus pneumoniae*: identification of clones associated with serious invasive disease. *Microbiology* 1998;144(Part 11):3049–60.
- [52] Dorak MT. Real-time PCR. New York; Abingdon [England]: Taylor & Francis; 2006.
- [53] Finkelstein JA, Huang SS, Daniel J, Rifas-Shiman SL, Kleinman K, Goldmann D, et al. Antibiotic-resistant *Streptococcus pneumoniae* in the heptavalent pneumococcal conjugate vaccine era: predictors of carriage in a multicommunity sample. *Pediatrics* 2003;112(4):862–9.
- [54] Pfaffl MW. A new mathematical model for relative quantification in real-time RT-PCR. *Nucleic Acids Res* 2001;29(9):e45.
- [55] Fierer N, Jackson JA, Vilgalys R, Jackson RB. Assessment of soil microbial community structure by use of taxon-specific quantitative PCR assays. *Appl Environ Microbiol* 2005;71(7):4117–20.
- [56] Kais M, Spindler C, Kalin M, Ortqvist A, Giske CG. Quantitative detection of *Streptococcus pneumoniae*, *Haemophilus influenzae*, and *Moraxella catarrhalis* in lower respiratory tract samples by real-time PCR. *Diagn Microbiol Infect Dis* 2006;55(3):169–78.

- [57] Zheng G, Wang C, Williams HN, Pineiro SA. Development and evaluation of a quantitative real-time PCR assay for the detection of saltwater *Bacteriovorax*. *Environ Microbiol* 2008;10(10):2515–26.
- [58] Hausdorff WP, Bryant J, Paradiso PR, Siber GR. Which pneumococcal serogroups cause the most invasive disease: implications for conjugate vaccine formulation and use, part I. *Clin Infect Dis* 2000;30(1):100–21.
- [59] Casey JR, Adlowitz DG, Pichichero ME. New patterns in the otopathogens causing acute otitis media six to eight years after introduction of pneumococcal conjugate vaccine. *Pediatr Infect Dis J* 2009.
- [60] Casey JR, Adlowitz DG, Pichichero ME. New patterns in the otopathogens causing acute otitis media six to eight years after introduction of pneumococcal conjugate vaccine [Abstract #G-3]. In: Presented at the 48th Interscience Conference on Antimicrobial Agents and Chemotherapy. 2008.
- [61] Weinberger DM, Trzcinski K, Lu YJ, Bogaert D, Brandes A, Galagan J, et al. Pneumococcal capsular polysaccharide structure predicts serotype prevalence. *PLoS Pathog* 2009;5(6):e1000476.
- [62] Hall-Stoodley L, Hu F, Gieseke A, Nistico L, Nguyen D, Hayes J, et al. Direct detection of bacterial biofilms on the middle-ear mucosa of children with chronic otitis media. *JAMA* 2006;296(2):202–11.
- [63] Moscoso M, Garcia E, Lopez R. Biofilm formation by *Streptococcus pneumoniae*: role of choline, extracellular DNA, and capsular polysaccharide in microbial accretion. *J Bacteriol* 2006;188(22):7785–95.
- [64] Oggioni MR, Trappetti C, Kadioglu A, Cassone M, Iannelli F, Ricci S, et al. Switch from planktonic to sessile life: a major event in pneumococcal pathogenesis. *Mol Microbiol* 2006;61(5):1196–210.
- [65] Hava DL, Camilli A. Large-scale identification of serotype 4 *Streptococcus pneumoniae* virulence factors. *Mol Microbiol* 2002;45(5):1389–406.
- [66] Blomberg C, Dagerhamn J, Dahlberg S, Browall S, Fernebro J, Albiger B, et al. Pattern of accessory regions and invasive disease potential in *Streptococcus pneumoniae*. *J Infect Dis* 2009;199(7):1032–42.
- [67] Chonmaitree T, Revai K, Grady JJ, Clos A, Patel JA, Nair S, et al. Viral upper respiratory tract infection and otitis media complication in young children. *Clin Infect Dis* 2008;46(6):815–23.
- [68] Bakaletz LO, Daniels RL, Lim DJ. Modeling adenovirus type 1-induced otitis media in the chinchilla: effect on ciliary activity and fluid transport function of eustachian tube mucosal epithelium. *J Infect Dis* 1993;168(4):865–72.
- [69] Chung MH, Griffith SR, Park KH, Lim DJ, DeMaria TF. Cytological and histological changes in the middle ear after inoculation of influenza A virus. *Acta Otolaryngol* 1993;113(1):81–7.
- [70] Park K, Bakaletz LO, Cotichia JM, Lim DJ. Effect of influenza A virus on ciliary activity and dye transport function in the chinchilla eustachian tube. *Ann Otol Rhinol Laryngol* 1993;102(7):551–8.
- [71] Suzuki K, Bakaletz LO. Synergistic effect of adenovirus type 1 and nontypeable *Haemophilus influenzae* in a chinchilla model of experimental otitis media. *Infect Immun* 1994;62(5):1710–8.
- [72] Giebink GS, Berzins IK, Marker SC, Schiffman G. Experimental otitis media after nasal inoculation of *Streptococcus pneumoniae* and influenza A virus in chinchillas. *Infect Immun* 1980;30(2):445–50.
- [73] Revai K, Dobbs LA, Nair S, Patel JA, Grady JJ, Chonmaitree T. Incidence of acute otitis media and sinusitis complicating upper respiratory tract infection: the effect of age. *Pediatrics* 2007;119(6):e1408–12.
- [74] Gillespie SH. Antibiotic resistance in the absence of selective pressure. *Int J Antimicrob Agents* 2001;17(3):171–6.
- [75] Edwards K, Logan J, Saunders N. *Horizon bioscience. Real-time PCR: an essential guide*. Wymondham, Norfolk: Horizon Bioscience; 2004.
- [76] Rayner MG, Zhang Y, Gorry MC, Chen Y, Post JC, Ehrlich GD. Evidence of bacterial metabolic activity in culture-negative otitis media with effusion. *JAMA* 1998;279(4):296–9.
- [77] Post JC, Aul JJ, White GJ, Wadowsky RM, Zavoral T, Tabari R, et al. PCR-based detection of bacterial DNA after antimicrobial treatment is indicative of persistent, viable bacteria in the chinchilla model of otitis media. *Am J Otolaryngol* 1996;17(2):106–11.
- [78] Ehrlich GD, Hu FZ, Shen K, Stoodley P, Post JC. Bacterial plurality as a general mechanism driving persistence in chronic infections. *Clin Orthop Relat Res* 2005;437(437):20–4.
- [79] Baba T, Takeuchi F, Kuroda M, Yuzawa H, Aoki K, Oguchi A, et al. Genome and virulence determinants of high virulence community-acquired MRSA. *Lancet* 2002;359(9320):1819–27.
- [80] Fux CA, Shirliff M, Stoodley P, Costerton JW. Can laboratory reference strains mirror “real-world” pathogenesis? *Trends Microbiol* 2005;13(2):58–63.